Electron- and light microscopic distribution of AQP4 in mouse substantia nigra

Nina Davarpaneh and Maria Nadeem

Supervisors
Katja Stahl
Mahmood Amiry-Moghaddam

Research project for Medical students
Faculty of Medicine

UNIVERSITY OF OSLO

04.10.13

Abstract

Background: Aquaporin 4 (AQP4) is the predominant water channel in the brain and is localized to the astrocytes and ependymal cells. In astrocytes it is expressed in the astrocyte membranes facing blood vessels and pia in a highly polarized manner. This polarization has been demonstrated to be important in the water and K^+ homeostasis. Several studies indicate that the polarized expression of AQP4 has an important role in the pathophysiology of several cerebral disorders, including brain edema, epilepsy and Alzheimer's disease.

Objective: In this study, we want to investigate the distribution and expression pattern of AQP4 in mouse substantia nigra (SN). AQP4 has not been explored in this area previously. By examining its distribution, we want to see whether AQP4 could have a role in the neuronal function in this area under normal and pathological conditions

Methods: We investigated the AQP4 distribution in the SN and neocortex of C57BL/6 mice. The animals were perfusion fixed and brains analyzed using confocal immunofluorescence and quantitative immunogold electron microscopy.

Results: We found significantly higher levels of AQP4 in the SN, as compared to the neocortex. The AQP4 expression was highly polarized around blood vessels, both in the pars compacta and pars reticulata. There was also substantially more AQP4 in astrocyte processes throughout the neuropil in the SN compared to the neocortex.

Conclusion: The high expression of AQP4 in both endfeet and non-endfeet membranes indicate that this molecule might play an important role for maintenance of neuronal function in the SN. Studying expression pattern of AQP4 in mouse models of Parkinson's disease may give additional information about its functional significance.

Introduction

Aquaporins are a family of water channels that facilitate water transport across plasma membranes (1). Aquaporins have been identified in mammals, invertebrates, microbials and plants. In mammals there has been identified at least 10 aquaporins which are selectively permeated by water or water plus glycerol (2). One member of this family, Aquaporin 4 (AQP4), is the predominant water channel in the brain. It is expressed in the brain neuropil where it is localized to astrocytes and ependymal cells. In astrocytes, it has a highly polarized expression at membrane areas facing blood vessels and pia. AQP4 is heavily expressed in the osmosensory areas of the brain, including the hypothalamic magnocellular nuclei and the subfornical area (3), and in astrocytes it forms a volume regulatory complex with the Transient receptor potential cation channel subfamily 4 (TRPV4) indicating that it is involved in the brain volume water homeostasis (4). In addition, there is also evidence that AQP4 is associated with K^+ homeostasis. Amiry-Moghaddam et al. have shown that a loss of astrocyte polarity delays the K^+ clearance during high neuronal activity in animal model where α-syntrophin, an AQP4 anchoring protein, is deleted (5).

AQP4 is involved in the pathophysiology of several cerebral disorders, including epilepsy, brain edema and Alzheimer's disease. Amiry-Moghaddam et al. reported that mice with the loss of astrocyte polarity reveal increased severity of induced seizures (5). Loss of the perivascular AQP4 has been reported in the sclerotic areas of human hippocampus in temporal lobe epilepsy (6).In addition, there are several studies reporting a role of AQP4 in the pathophysiology of brain edema. One of the first studies on this topic reported that mice deficient in AQP4 had a much better survival than wild-type mice, in models of brain edema caused by acute water intoxication or focal ischemic stroke (7). Regarding the role of AQP4 in the pathogenesis and pathophysiology of Alzheimer's disease, it was shown that perivascular amyloid deposits lead to the decrease of perivascular AQP4 labeling. This loss of astrocyte polarization was likely to have impact on brain function (8). In addition to these cerebral diseases there have recently been reports of the importance of AQP4 in the pathophysiology of Parkinson's disease (PD). It was reported in a study that mice deficient in AQP4 had an increased sensitivity of dopaminergic neurons to 1-methyl-4-phenyl-1,2,3,6-tetrahydropyrin (MPTP), a nigrostriatal dopaminergic neurotoxin which causes a PD-like syndrome (9). It was further discovered that AQP4 deficiency disrupts the immunosuppressive regulators, resulting in hyperactive microglial neuroinflammatory responses in the brain, possibly contributing to the increased severity of PD (10). This result showed that not only is AQP4 important in the water and K^+ homeostasis, but could also have and important role in the immunological processes in brain.

AQP4, as mentioned, has an important role in the pathophysiology of several cerebral disorders, and the distribution of this water channel has been reported in previous studies. It is already known that there are lower number of astrocytes in the substantia nigra (SN) than in other areas of the brain, and that this could be an explanation for the increased susceptibility of the dopamine neurons in nigra (11). There is still little information of the distribution of AQP4 in SN. With this study, we want to investigate the distribution and expression pattern of AQP4 in the SN as compared to the neocortex of mice by the use of confocal microscopy- and quantitative immunogold electron microscopy. This area has still not been explored and the results from this study can help to understand what role AQP4 can have in the neuronal function in SN.

Materials and methods

All chemicals used, except for those specified in the text, were from Sigma-Aldrich, Norway.

Animals

Five C57BL/6, 6-8 weeks old all of male gender, were used for light microscopy and three C57BL/6, 12 weeks old all of male gender for electron microscopy. Experimental protocols were approved by the Institutional Animal Care and Use Committee and conform to National Institutes of Health guidelines for the care and use of animals.

Perfusion and dissection

Before dissection and perfusion, each animal was anesthetized by an intraperitoneal injection of hypnorm dormicum (0.105 mg/kg). After making sure the animal was adequately anesthetized, it was fixed lying on its back to a board. Some ethanol was applied to the abdomen and then a midline incision was made into the peritoneal cavity. The incision continued laterally exposing the heart and lungs. A small incision was made in the right atrium, and then a cannula was inserted in the left ventricle. Animals for use in light microscopy were perfused using pH shift-protocol (12). In brief, the animal was first perfused with 2 % ice cold dextran solution for 20 sec then switched to 4 % formaldehyde (FA) in phosphate buffer (PB), pH 6.0, for 5 min, before ending with 4 % FA in PB, pH 10.5, for 10 min. Following perfusion, brains were dissected out and post-fixed in 4 % FA overnight. The brains were then cryoprotected in sucrose, 10% for 1 hour, 20 % for 6 hours and 30 % overnight. From each animal, the midbrain was isolated and cut into 30 µm sections using a HM 450 freeze microtome (Microm, Walldorf, Germany).

For electron microscopy, all animals were perfusion fixed with 4 % FA and 0.1 % glutaraldehyde and post-fixed in the same solution overnight. 1x1 mm tissue blocks of parietal cortex and SN were dissected and subjected to freeze substitution procedure (13). In brief, the tissue blocks were cryoprotected in glycerol and rapidly frozen in liquid propane at -170ºC. The frozen tissue was immersed into anhydrous methanol containing 0,5 % uranyl acetate at -90ºC in an automatic freeze substitution unit (EMAFS, Leica, Vienna, Austria), infiltrated with Lowicryl HM20 Resin (Lowy, Waldkraiburg, Germany) at -30ºC, polymerized by ultraviolet light, sectioned ultrathin 90-100 nm using ultramicrotome, transferred to mesh grids, and used for immunogold labeling.

Antibodies

In order to immunolabel dopaminergic cells a mouse monoclonal antibody against tyrosine hydroxylase (TH) was used (Chemicon, Billerica, MA, USA). It was diluted to a concentration of 1:1000. To visualize the primary antibody, Cy2- or Alexa488-conjugated donkey anti-mouse secondary antibodies were used (West Grove, PA, USA). All the secondary antibodies were diluted 1:1000.

For immunolabeling of AQP4 a rabbit polyclonal antibody raised against the C-terminus of AQP4 was used (Sigma-Aldrich). This was diluted 1:200. For immunofluorescence light microscopy, Cy3- or Cy5-conjugated donkey anti-rabbit secondary antibodies were used

(Jackson ImmunoResearch Laboratories). For immunogold labeling, a goat polyclonal secondary antibodies to rabbit IgG coupled to 15 nm gold particles (1:20, Abcam, Cambridge) was used as the secondary antibody.

Immunofluorescence and confocal microscopy

Blocking

Immunofluorescence was performed on free-floating sections according to a method previously described (14). The sections were transferred to separate wells containing 0.01M phosphate buffered saline (PBS; 137mM NaCl, 2.7mM KCl, 10.1mM Na_2HPO_4, 1.8mM KH_2PO_4, pH 7.4) and rinsed for 2x10 minutes. To minimize unspecific binding, the sections were then blocked for one hour in pre-incubation solution, containing 10 % normal goat serum (NGS), 1 % bovine serum albumin (BSA) and permeabelized with 1 % Triton-X-100 in 0.01M PBS to improve antibody penetration in the tissue.

Incubation with primary antibodies

The primary antibodies (see above) were diluted in primary incubation solution, containing 3 % NCS, 1 % BSA, 1 % Triton-X-100 and 0.05 % sodium azide in 0.01M PBS. The sections were incubated with the primary antibodies overnight in room temperature.

Incubation with secondary antibodies

The following day, the sections were rinsed in 0.01M PBS 3x10 minutes to wash off excessive antibodies. The tissues were then incubated with secondary antibodies (see above) for one hour. Secondary antibodies were diluted in a secondary incubation solution, containing 3 % NCS, 1 % BSA and 1 % Triton X-100 in 0.01M PBS. The secondary antibodies and the final solution containing the secondary antibodies were centrifuged at 13000 rpm for 10 minutes before use to avoid aggregates. During all the steps the secondary antibodies and the final solution were covered with tin foil due to light sensitivity of the dyes. After incubations with the secondary antibodies, the sections were again rinsed in 0.01M PBS for 3x10 minutes.

Mounting of sections

The sections were placed on a cover glass and excess PBS was removed by tapping on a paper towel. A small drop of Prolong Gold Antifade Reagent with DAPI (Invitrogen, Norway) was added on top of the tissue in order to stain DNA of all cells in the specimen. The sections were covered with a coverslip and allowed to dry in room temperature for two hours.

Confocal microscopy

A confocal microscope collects light from a thin optical section at the plane of focus in the specimen. Structures appear more sharply defined than with a conventional microscope

because there is no out-of-focus signal (15). Images were collected with a LSM 510 META Confocal Microscope (Zeiss, Jena, Germany) using a 40 x objective. Cy3 fluorescence was captured at 568 nm, Alexa 488 at 510 nm, Cy5 at 670nm and DAPI at 405 nm.

Immunogold electron microscopy

For quantitative immunogold studies, Lowicryl embedded blocks from the neocortex and SN was cut into ultrathin sections using an ultratome (Leica EM UC6, Austria). The ultrathin sections were then placed on nickel grids and incubated in drops of Tris-buffered saline with 0.1% triton (TBST) and 50 mM glycine for 10 minutes, washed in water and then incubated for 10 minutes in drops of TBST containing 2 % w/v human serum albumin (HSA). The grids were then incubated in a solution of 2 % w/v HSA, TBST and anti-AQP4 over night at room temperature. The labeling was visualized with goat anti-rabbit IgG antibodies coupled to 15 nm colloidal gold particles diluted in 1:20 TBST with 2 % w/v HSA and polyethylene glycol. The sections were contrasted with 1 % uranyl acetate and lead citrate and finally examined with electron microscope (Tecnai 12, FEI Company, Eindhoven, the Netherlands). 25-30 blood vessels from each section (16 bit) were selected at low magnification, and one image was acquired from upper right corner of each capillary with a 25000x magnification.

Quantification and statistical analysis

For the quantification of AQP4, images from capillaries were selected in a blinded manner from each section and quantified with an image analysis program, analysis Pro version 3.2 (soft imaging system GmbH, Munster, Germany). Larger vessels and distorted or mechanically damaged basal lamina were excluded. Curves were drawn interactively, and linear densities were determined automatically. Groups were analyzed statistically by t-tests using SPSS version 18.0. The significance level was set to 0.05.

Results

Controls

Negative controls from SN for immunofluorescence light- and immunogold electron microscopy were performed by incubating the sections in only secondary antibodies. In addition, there was also used AQP4 knockout (KO) for immunogold electron microscopy (Fig. 1). In absence of the primary antibodies, the secondary antibodies did not reveal any labeling, indicating the specificity of the antibodies.

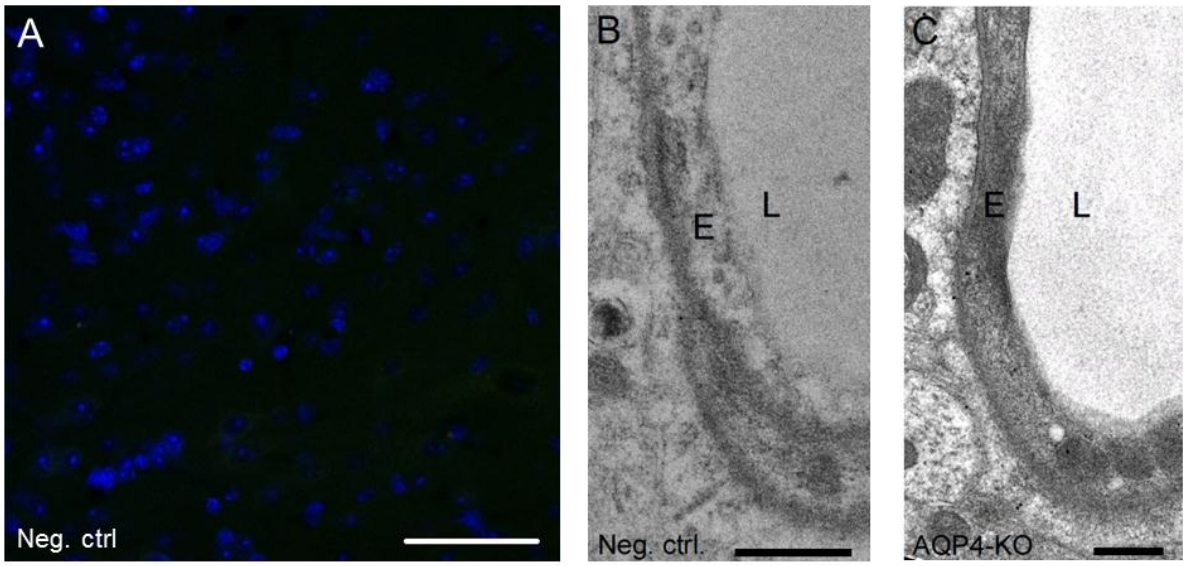

Fig. 1. Specificity controls for the antibodies.
A-B) The sections were only incubated with secondary antibodies. For immunofluorescence light microscopy (A), Alexa488 and Cy3 were used as secondary antibodies. The nuclei were labeled with DAPI (blue). For immunogold electron microscopy (B), goat polyclonal antibodies against rabbit IgG coupled to 15 nm gold particles. C) Sections from AQP4-KO mouse brain was incubated with both anti-AQP4 and secondary antibodies. There is no labeling of AQP4 and TH indicating the specificity of the antibodies. *E*, endothelial cells; *L*, lumen of capillary. Scale bars: *A*, 50 µm; *B* and *C*, 1 µm.

Immunofluorescence analysis

To know whether or not the area being analyzed in fact was SN, TH labeling was used as an indication. TH is an enzyme exclusively expressed in catecholaminergic neurons. Dopaminergic cells are the main catecholaminergic cell groups in the midbrain. By isolating the midbrain we can assume that the accumulation of TH labeled cells from this area indicates dopaminergic neurons located to SN.

Immunofluorescence analysis of the superficial layer of the neocortex showed evident labeling of AQP4 around blood vessels and at the pial surface (Fig. 2A). This polarization of AQP4 around blood vessels is in accordance with findings in a previous study (3). When examining the deeper layer of the neocortex the findings was in keeping with the superficial area, showing that the AQP4 labeling was concentrated around blood vessels (Fig.2B). In both the superficial and the deeper layer of the neocortex there was no labeling of AQP4 elsewhere in the neuropil (Fig. 2A and 2B).

Immunofluorescence analysis of SN pars compacta showed strong AQP4-labeling that was highly polarized around blood vessels (Fig. 2C and 2D). In addition to this polarization, diffuse AQP4 labeling in the non-endfeet membranes throughout the neuropil was also evident (Fig. 2C and 2D). Analysis of SN pars reticulata showed the same distribution pattern as seen in pars compacta, with excessive AQP4 labeling concentrated around blood vessels, and also a high intensity of AQP4 labeling throughout the neuropil (Fig. 2E and 2F).

Quantitative immunogold electron microscopy

In agreement with our immunofluorescence labeling, electron micrograph images showed significantly higher immunolabeling in SN compared to the neocortex (Fig. 3A). AQP4 labeling is highly polarized around perivascular membranes (Fig. 3A). In addition to this polarization, AQP4 labeling was also evident in the non-endfeet membranes. SN sections revealed higher density of gold particles in non-endfeet membranes compared to the neocortex.

The quantitative analysis showed significantly higher perivascular gold particle density in astrocyte membrane domains of the SN compared to neocortex (Fig. 3C). The linear density of gold particles along perivascular membranes was 70 % higher in the SN as compared to neocortex, with a mean density of 28.4 ± 1.0 gold particles for SN as compared to 16.8 ± 0.7 for cortex (Values are mean ± SEM).

The non-endfeet labeling was measured as areal density of gold particles in randomly selected images from neuropil. The quantitative analysis revealed a 135 % higher gold particle density in the SN compared to neocortex, with a mean density of 12.7 ± 1.6 gold particles for SN as compared to 5.5 ± 0.5 for cortex (Fig. 3D) (Values are mean ± SEM). This is in line with our immunofluorescence observation of the diffuse AQP4 labeling in neuropil (Fig. 2).

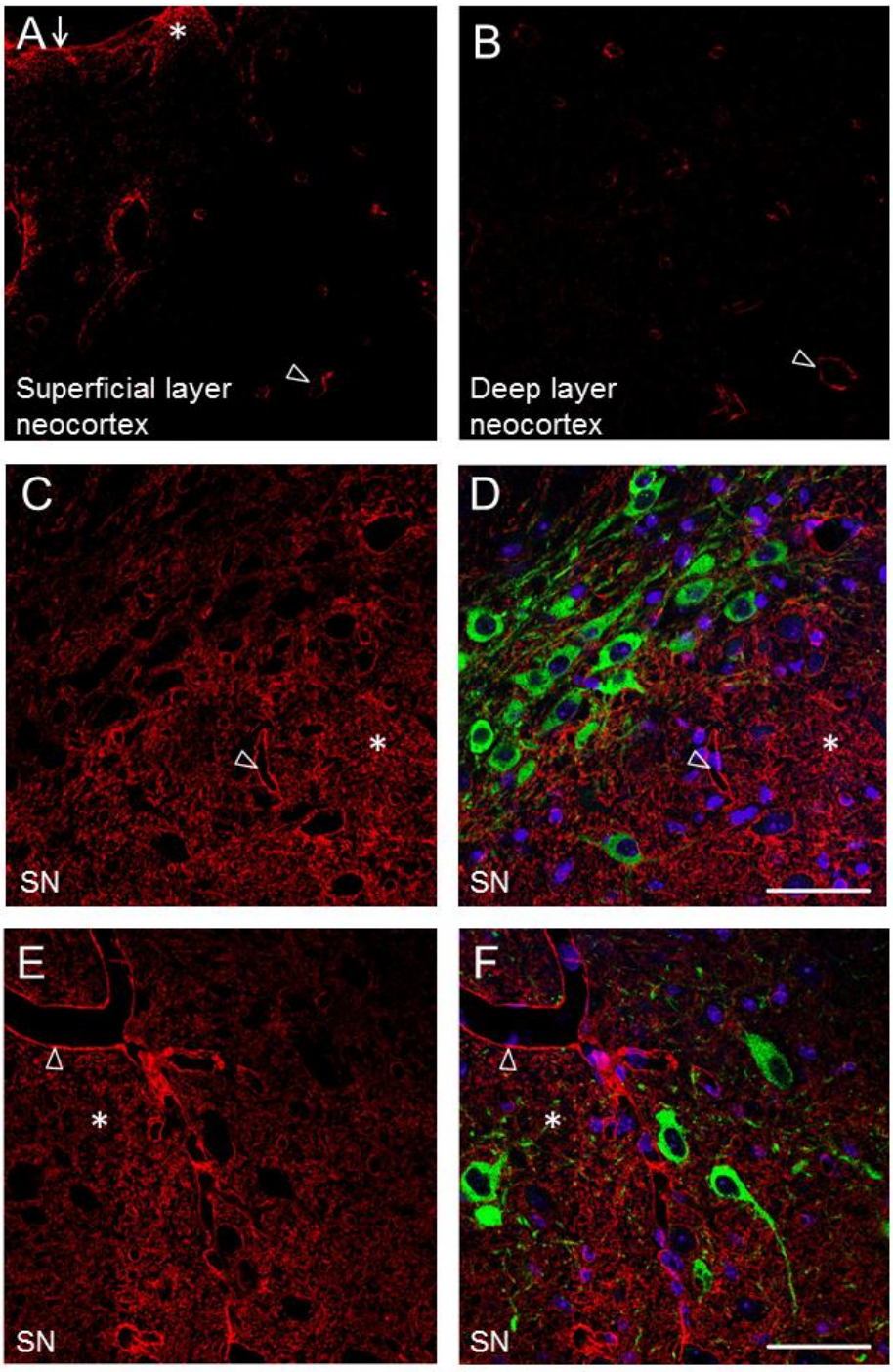

Fig. 2. Immunofluorescence images from neocortex and substantia nigra.

A) In the superficial layers of neocortex, AQP4-labeling is evident at the pial surface and around some blood vessels. B) In deeper layers of the neocortex, the AQP4-labeling is restricted to blood vessels. C-D) The substantia nigra pars compacta show excessive labeling of AQP4 (red), particularly around blood vessels, but also throughout the neuropil. TH-positive cells are seen in green and nuclear DAPI-staining in blue. E-F) A similar pattern of AQP4 is seen at the border between pars compacta and pars reticulata. *Arrow*, pial surface; *Arrowheads,* perivascular labeling; *Asterisks,* AQP4 labeling in the non-endfeet membranes; *SN*, substantia nigra. Scale bar 50 µm.

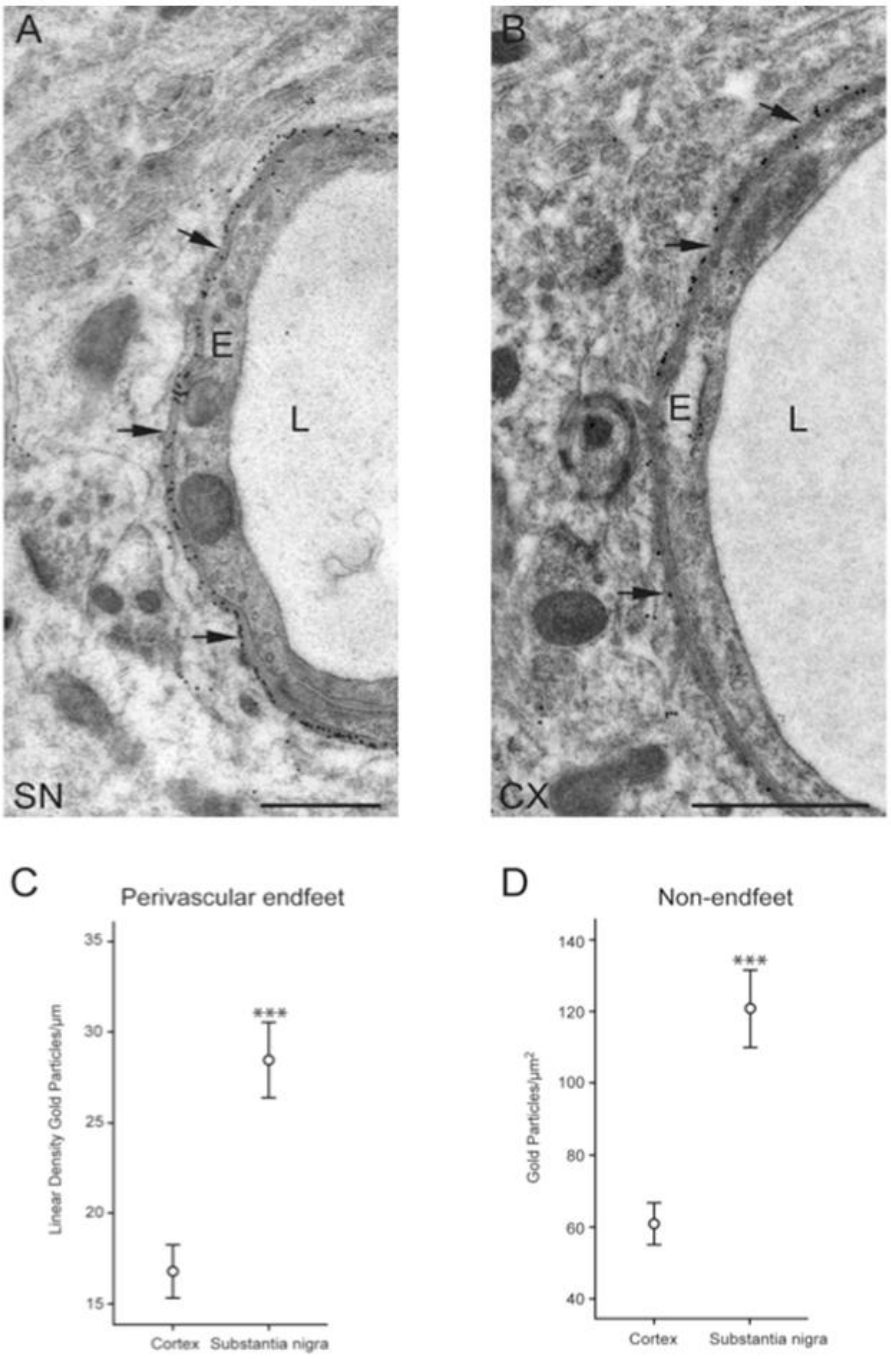

Fig. 3. Quantitative immunogold analysis of substantia nigra and neocortex.

A-B) Electron micrographs showing AQP4 immunogold labeling (15 nm gold particles). A) In the substantia nigra, AQP4-labeling is highly polarized around perivascular processes (single arrows). B) The neocortex show lower density of AQP4 immunogold labeling as compared to the substantia nigra, both at perivascular membranes and throughout the neuropil. C-D) Quantitation of AQP4 in the substantia nigra and neocortex at perivascular endfeet membrane (C) and non-feet membranes (D) demonstrate a significant difference in both linear density (C) and density class of gold particles (D), with higher density of AQP4 immunogold particles in substantia nigra compared to the neocortes, $p>0.001$. *SN*, Substantia nigra; *CX*, neocortex; *E*, endothelial cell; *L*, lumen of capillary. Scale bar 1 µm.

Discussion

AQP4 is a water channel with high expression in the brain (16). It consists of four individually functional monomers that span the cell membrane 6 times and assemble into tetramers with a central pore (17). The main localization of AQP4 has been shown to be to the astrocyte membrane domains facing blood vessels and pia (3). However, there has been no investigation of the distribution and expression of AQP4 in the SN. The present study is the first to do so. The key finding in this study is a significantly higher density of AQP4 labeling in the perivascular membranes as well as in the non-endfeet membranes of neuropil in the SN as compared to the neocortex.

In this study we used both immunofluorescence and immunogold analysis for investigating the distribution and expression of AQP4. Immunofluorescence analysis provides a qualitative indication of the AQP4 distribution pattern in the SN. A fluorescently labeled secondary antibody directed against the primary antibody towards AQP4, enables us to visualize AQP4 in a highly specific way (18). Further, this method allows us to label different proteins within the same tissue. By being able to label both AQP4 and TH in the same tissue, the distribution pattern can be assessed more precisely as localization of AQP4 is shown in relation to other cells. This quality of dual labeling adds to the qualitative function of this method (19). However, this method does not provide high resolution, making it difficult to quantify and to assess the precise localization of AQP4. This is possible by the use of immunogold labeling. Gold particles can be discriminated with high resolution by electron microscopy. This allows us to visualize the localization of AQP4 with high precision. Further, the gold particles are easy to identify in an electron microscope, therefore easily counted, making this method suitable for quantification (20). Together, the qualitative immunofluorescence and quantitative immunogold labeling analysis in this study confirm the presence of strong labeling around microvessels in the neocortex and SN with a diffuse immunostaining in the parenchyma in the SN not present in the neocortex.

The perivascular labeling of AQP4 in the immunofluorescence analysis is evident. However, it would have been ideal to have markers for endothelial cells in blood vessels in order to visualize the relation of AQP4 to the blood vessels more precisely. In addition, it would have been beneficial to have an AQP4-KO mouse in the immunofluorescence analysis. In knockout animals you remove the antigen that the primary antibody is directed against making this a good specificity control for the primary antibody, as opposed to negative controls which primarily test the secondary antibodies (21). An AQP4-KO mouse in the immunofluorescence analysis would add to the controls showing the specificity of the antibodies. Further, in this study we used primary antibodies directed towards the C-terminus. By immunostaining with antibodies directed towards other areas of the molecule, like the N-terminus, we would be even more confident that the structure being analyzed in fact is AQP4 (18). Although this would be the ideal situation, we still have a high level of certainty of the results in this study. By using immunofluorescence in combination with high-resolution immunogold labeling analysis we confirm that AQP4 molecules are in fact located to the perivascular membrane. Regarding the diffuse labeling of AQP4 in immunofluorescence, the localization to the non-endfeet membranes of the neuropil is confirmed in immunogold analysis. We also show the high level of specificity of the antibodies by using negative controls in both methods and sections from AQP4-KO mouse brain in the immunogold analysis.

Before we go further and discuss the role of AQP4 in SN, the role of astrocytes generally and in SN specifically should be addressed. It is known that astrocytes form a heterogeneous population, although not much is known about the specific properties of astrocytes in the SN (22). Astrocytes generally have many functions including maintenance of extracellular ion and water balance and the regulation of blood flow (23, 24). We can assume that astrocytes in SN have similar functions as the rest of brain. Noteworthy, the number of astrocytes in SN is found to be particularly low as compared to other brain areas (11). Our findings demonstrate a significantly higher expression of AQP4 in the SN when compared to the neocortex, leading us to speculate whether the small population of astrocytes located in the SN entails specific properties related to AQP4 expression. Possibly, these astrocytes may express more AQP4 per cell as compared to astrocytes found elsewhere in the brain.

Astrocytes have a neuroprotective role due to their capacity to reduce free radicals and secrete neuroprotective factors (11). Normal metabolism of dopamine generates reactive oxygen species (ROS), which provides an endogenous source of oxidative stress. Thus, a smaller proportion of astrocytes in the SN protecting the dopamine neurons against ROS could be an explanation for the increased susceptibility of the dopamine neurons in SN seen in PD. High levels of monoamine oxidase B (MAO-B) in this area is another factor making SN more disposed (25). The oxidative degradation of dopamine, catalyzed by MAO-B, produces free radicals, which increases oxidative stress and can be damaging to neighboring neurons. The SN also appears to be disposed to inflammatory processes. Elevated levels of intercellular adhesion molecule-1 (ICAM-1) (26), an inflammatory mediator, has been found in astrocytes in the SN which may make this region more vulnerable to inflammation.

As mentioned, dopamine is capable of producing toxic ROS via its enzymatic catabolism, which can have damaging effect on the brain tissue (27, 28). Possibly, the high expression of AQP4 in the SN observed in this study may be a response to this high level of free radicals. We know that extracellular space (ECS) volume changes can have an impact on the concentration of extracellular solutes (29). Further, it is shown that AQP4, with bidirectional water transport, has a role in regulating this ECS volume in the brain (30, 31). By increasing the ESC volume, AQP4 can reduce concentration of the free radicals, thereby reducing the damaging effect. In addition to this indirect function of dilution, it could also be possible that these water channels have a more direct transportation function. Aquaporins are generally known for water transport and Fenton et al. have shown that the monomers are mainly permeable to water molecules (1, 32). However, their involvement in permeation of molecules other than water has been suggested (33). Recently, there have been reports of permeability of molecules in the central pore of aquaporins. Musa-Aziz et al. have through their study demonstrated that water, cations and gases, such as CO2, flow through the central pore (34). Potentially, the large amount of free radicals in SN can flow through the central pore signifying the need of high density of AQP4 in SN compared to other regions of the brain.

The suggestion that AQP4 can have a role in transportation of other molecules than water is a recent discovery. However the role of AQP4 in transportation of water is well established. It could be a hypothesis that excessive water production in the SN could be a reason for the abundant labeling of AQP4. Dopaminergic cells in SN have a high level of metabolic activity due to the synthesis of dopamine. It could be speculated that excessive AQP4 in SN signifies a need for transport of water produced from this high metabolic activity. Further, the high level of AQP4 in SN could also be explained by the water transport from the glucose metabolism, which is the main energy fuel in the brain. During glucose metabolism, excessive

amounts of water is produced (35). Possibly, there could be high glucose utilization in this area because of high metabolic activity, indicating the need for AQP4 to flux water produced from this glucose metabolism. However, studies have shown that the utilization of glucose in the SN is lower compared to the cerebral cortex, making this hypothesis unlikely (36).

AQP4 has proven to be particularly important for regulation of K^+ homeostasis (5). Studies on retinal Müller cells have shown a coupling of AQP4 to Kir4.1, a K^+ channel known to have a role in the clearance of extracellular K^+ (37). Further studies have shown that other astrocytes have the same property in K^+ clearance as the Müller cells (38). During neuronal activity there is an increase of extracellular K^+. Efficient clearance of this extracellular K^+ is required to avoid interference with neuronal signaling (39). Studies have shown that there are regional differences in extracellular potassium levels in the brain (40). Possibly, there could be a higher level of extracellular potassium in SN compared to cortex because of the metabolic activity in dopaminergic cells. Thus, the high level of AQP4 in SN could be a response to the increased extracellular K^+ from this high metabolic activity.

The results in this paper indicate that AQP4 might play an important role for maintenance of neuronal function in the SN. It is already known that AQP4 is involved in the pathophysiology of several cerebral disorders, including epilepsy, brain edema and Alzheimer's disease. A common feature for these cerebral disorders is loss of astrocyte polarization, which is known to compromise astrocyte function (8). It would be interesting to see if a similar or different pattern is found in a PD mouse model. As by now, the expression of AQP4 in animal models of PD has not been studied. Recently, in an MTPT-induced mouse model of PD, AQP4 deficient animals showed more microglial inflammatory responses and more severe loss of dopaminergic neurons compared to wild type mice (10). They also showed signs of more severe PD symptoms than their wild type littermates. Further, we have raised some questions throughout our discussion. For instance, is the ECS volume in SN larger compared to other areas of the brain and does it lead to dilution of toxins? In the future, it would be very interesting to characterize the expression patterns of AQP4 in animal models of PD and to study its potential role in the PD pathophysiology. Future studies should also address the possible role of the ECS volume in removing toxins in SN.

Acknowledgments

We thank Katja Stahl and Mahmood Amiry-Moghaddam for supervision, training in how to conduct the experiments and giving valuable comments on this paper. We also thank Bjørg Riber and Carina V. Knudsen for technical assistance.

References

1. Agre P, Preston GM, Smith BL, Jung JS, Raina S, Moon C, et al. Aquaporin CHIP: the archetypal molecular water channel. The American journal of physiology. 1993 Oct;265(4 Pt 2):F463-76.
2. Agre P, King LS, Yasui M, Guggino WB, Ottersen OP, Fujiyoshi Y, et al. Aquaporin water channels--from atomic structure to clinical medicine. The Journal of physiology. 2002 Jul 1;542(Pt 1):3-16.
3. Nielsen S, Nagelhus EA, Amiry-Moghaddam M, Bourque C, Agre P, Ottersen OP. Specialized membrane domains for water transport in glial cells: high-resolution immunogold cytochemistry of aquaporin-4 in rat brain. The Journal of neuroscience : the official journal of the Society for Neuroscience. 1997 Jan 1;17(1):171-80.
4. Benfenati V, Caprini M, Dovizio M, Mylonakou MN, Ferroni S, Ottersen OP, et al. An aquaporin-4/transient receptor potential vanilloid 4 (AQP4/TRPV4) complex is essential for cell-volume control in astrocytes. Proceedings of the National Academy of Sciences of the United States of America. 2011 Feb 8;108(6):2563-8.
5. Amiry-Moghaddam M, Williamson A, Palomba M, Eid T, de Lanerolle NC, Nagelhus EA, et al. Delayed K+ clearance associated with aquaporin-4 mislocalization: phenotypic defects in brains of alpha-syntrophin-null mice. Proceedings of the National Academy of Sciences of the United States of America. 2003 Nov 11;100(23):13615-20.
6. Eid T, Lee TS, Thomas MJ, Amiry-Moghaddam M, Bjornsen LP, Spencer DD, et al. Loss of perivascular aquaporin 4 may underlie deficient water and K+ homeostasis in the human epileptogenic hippocampus. Proceedings of the National Academy of Sciences of the United States of America. 2005 Jan 25;102(4):1193-8.
7. Manley GT, Fujimura M, Ma T, Noshita N, Filiz F, Bollen AW, et al. Aquaporin-4 deletion in mice reduces brain edema after acute water intoxication and ischemic stroke. Nature medicine. 2000 Feb;6(2):159-63.
8. Yang J, Lunde LK, Nuntagij P, Oguchi T, Camassa LM, Nilsson LN, et al. Loss of astrocyte polarization in the tg-ArcSwe mouse model of Alzheimer's disease. Journal of Alzheimer's disease : JAD. 2011;27(4):711-22.
9. Fan Y, Kong H, Shi X, Sun X, Ding J, Wu J, et al. Hypersensitivity of aquaporin 4-deficient mice to 1-methyl-4-phenyl-1,2,3,6-tetrahydropyrindine and astrocytic modulation. Neurobiology of aging. 2008 Aug;29(8):1226-36.
10. Chi Y, Fan Y, He L, Liu W, Wen X, Zhou S, et al. Novel role of aquaporin-4 in CD4+ CD25+ T regulatory cell development and severity of Parkinson's disease. Aging cell. 2011 Jun;10(3):368-82.
11. Mena MA, Garcia de Yebenes J. Glial cells as players in parkinsonism: the "good," the "bad," and the "mysterious" glia. The Neuroscientist : a review journal bringing neurobiology, neurology and psychiatry. 2008 Dec;14(6):544-60.
12. Berod A, Hartman BK, Pujol JF. Importance of fixation in immunohistochemistry: use of formaldehyde solutions at variable pH for the localization of tyrosine hydroxylase. The journal of histochemistry and cytochemistry : official journal of the Histochemistry Society. 1981 Jul;29(7):844-50.
13. van Lookeren Campagne M, Oestreicher AB, van der Krift TP, Gispen WH, Verkleij AJ. Freeze-substitution and Lowicryl HM20 embedding of fixed rat brain: suitability for immunogold ultrastructural localization of neural antigens. The journal of histochemistry and cytochemistry : official journal of the Histochemistry Society. 1991 Sep;39(9):1267-79.
14. Stahl K, Skare O, Torp R. Organotypic cultures as a model of Parkinson s disease. A twist to an old model. TheScientificWorldJournal. 2009;9:811-21.

15. Smith CL. Basic confocal microscopy. Current protocols in neuroscience / editorial board, Jacqueline N Crawley [et al]. 2011 Jul;Chapter 2:Unit 2
16. Jung JS, Bhat RV, Preston GM, Guggino WB, Baraban JM, Agre P. Molecular characterization of an aquaporin cDNA from brain: candidate osmoreceptor and regulator of water balance. Proceedings of the National Academy of Sciences of the United States of America. 1994 Dec 20;91(26):13052-6.
17. Amiry-Moghaddam M, Ottersen OP. The molecular basis of water transport in the brain. Nature reviews Neuroscience. 2003 Dec;4(12):991-1001.
18. Polak JM, Van Noorden S. Introduction to immunocytochemistry. 3rd ed. Oxford: BIOS Scientific Publishers; 2003. xv, 176 p. p.
19. Hibbs AR. Confocal microscopy for biologists. New York: Kluwer Academic/Plenum Publishers; 2004. xiii, 467 p. p.
20. Amiry-Moghaddam M, Ottersen OP. Immunogold cytochemistry in neuroscience. Nature neuroscience. 2013 Jul;16(7):798-804.
21. Burry RW. Controls for immunocytochemistry: an update. The journal of histochemistry and cytochemistry : official journal of the Histochemistry Society. 2011 Jan;59(1):6-12.
22. Bachoo RM, Kim RS, Ligon KL, Maher EA, Brennan C, Billings N, et al. Molecular diversity of astrocytes with implications for neurological disorders. Proceedings of the National Academy of Sciences of the United States of America. 2004 Jun 1;101(22):8384-9.
23. Carmignoto G, Gomez-Gonzalo M. The contribution of astrocyte signalling to neurovascular coupling. Brain research reviews. 2010 May;63(1-2):138-48.
24. Koehler RC, Roman RJ, Harder DR. Astrocytes and the regulation of cerebral blood flow. Trends in neurosciences. 2009 Mar;32(3):160-9.
25. Damier P, Kastner A, Agid Y, Hirsch EC. Does monoamine oxidase type B play a role in dopaminergic nerve cell death in Parkinson's disease? Neurology. 1996 May;46(5):1262-9.
26. Morga E, Faber C, Heuschling P. Cultured astrocytes express regional heterogeneity of the immunoreactive phenotype under basal conditions and after gamma-IFN induction. Journal of neuroimmunology. 1998 Jul 1;87(1-2):179-84.
27. Sotomatsu A, Nakano M, Hirai S. Phospholipid peroxidation induced by the catechol-Fe3+(Cu2+) complex: a possible mechanism of nigrostriatal cell damage. Archives of biochemistry and biophysics. 1990 Dec;283(2):334-41.
28. Halliwell B. Reactive oxygen species and the central nervous system. Journal of neurochemistry. 1992 Nov;59(5):1609-23.
29. Strange K. Regulation of solute and water balance and cell volume in the central nervous system. Journal of the American Society of Nephrology : JASN. 1992 Jul;3(1):12-27.
30. Haj-Yasein NN, Jensen V, Ostby I, Omholt SW, Voipio J, Kaila K, et al. Aquaporin-4 regulates extracellular space volume dynamics during high-frequency synaptic stimulation: a gene deletion study in mouse hippocampus. Glia. 2012 May;60(6):867-74.
31. Amiry-Moghaddam M, Otsuka T, Hurn PD, Traystman RJ, Haug FM, Froehner SC, et al. An alpha-syntrophin-dependent pool of AQP4 in astroglial end-feet confers bidirectional water flow between blood and brain. Proceedings of the National Academy of Sciences of the United States of America. 2003 Feb 18;100(4):2106-11.
32. Fenton RA, Moeller HB, Zelenina M, Snaebjornsson MT, Holen T, MacAulay N. Differential water permeability and regulation of three aquaporin 4 isoforms. Cellular and molecular life sciences : CMLS. 2010 Mar;67(5):829-40.
33. Yu J, Yool AJ, Schulten K, Tajkhorshid E. Mechanism of gating and ion conductivity of a possible tetrameric pore in aquaporin-1. Structure. 2006 Sep;14(9):1411-23.

34. Musa-Aziz R, Chen LM, Pelletier MF, Boron WF. Relative CO2/NH3 selectivities of AQP1, AQP4, AQP5, AmtB, and RhAG. Proceedings of the National Academy of Sciences of the United States of America. 2009 Mar 31;106(13):5406-11.
35. Lieberman M, Marks AD, Smith CM. Marks' basic medical biochemistry : a clinical approach. 3rd ed. Philadelphia: Wolters Kluwer/Lippincott Williams & Wilkins; 2009. x, 1011 p. p.
36. Hawkins R, Hass WK, Ransohoff J. Measurement of regional brain glucose utilization in vivo using [2(-14)C] glucose. Stroke; a journal of cerebral circulation. 1979 Nov-Dec;10(6):690-703.
37. Nagelhus EA, Horio Y, Inanobe A, Fujita A, Haug FM, Nielsen S, et al. Immunogold evidence suggests that coupling of K+ siphoning and water transport in rat retinal Muller cells is mediated by a coenrichment of Kir4.1 and AQP4 in specific membrane domains. Glia. 1999 Mar;26(1):47-54.
38. Newman EA. High potassium conductance in astrocyte endfeet. Science. 1986 Jul 25;233(4762):453-4.
39. Somjen GG. Extracellular potassium in the mammalian central nervous system. Annual review of physiology. 1979;41:159-77.
40. Moghaddam B, Adams RN. Regional differences in resting extracellular potassium levels of rat brain. Brain research. 1987 Mar 17;406(1-2):337-40.